CIRP Annals - Manufacturing Technology 00 (2023) 1–4

Contents lists available at ScienceDirect

CIRP Annals - Manufacturing Technology

journal homepage: https://www.editorialmanager.com/CIRP/default.aspx

Inverse size effect and deformation mechanism in Ti-6Al-4V cutting process – investigation on effect of bimodal microstructure on machining

Shusong Zan[a], Guangyu Liu[b], Zhirong Liao (2)[a,*], Dragos Axinte (1)[a], Fengzhou Fang (1)[b,c]

[a] Machining and Condition Monitoring Group, Faculty of Engineering, University of Nottingham, NG8 1BB, UK
[b] State Key Laboratory of Precision Measuring Technology and Instruments, Laboratory of Micro/Nano Manufacturing Technology (MNMT), Tianjin University, Tianjin 300072, China
[c] Centre of Micro/Nano Manufacturing Technology (MNMT-Dublin), School of Mechanical and Materials Engineering, University College Dublin, Dublin 4, Ireland

ARTICLE INFO

Article history:
Available online xxx

Keywords:
Titanium
Machining

Ti-6Al-4 V finds wide applications in industrial areas due to its unique properties. Though, how its special microstructure (i.e., properties mismatch between different phases) could influence the surface/chip formation mechanism when machining (e.g., size effect) remains unclear. In this study, cutting experiments, simulation and post-processing materials characterizations of bimodal Ti-6Al-4 V were performed. Two interesting new phenomena were revealed: (i) variation of chip segmentation mechanism from regular serrated chip to serration at phase boundary when undeformed chip thickness reduces, (ii) 'inverse size effect' of specific shear energy. These findings open a new window of optimizing machining parameters for this specific material.

1. Introduction

Ti-6Al-4 V has been employed in many industry areas due to its superior properties (e.g., high strength to weight ratio, excellent corrosion resistance) [1,2]. However, its low thermal conductivity and high chemical reactivity result in high cutting temperature and short tool life which makes it to be classified as difficult-to-cut [2].

Although studies have been conducted on the machinability of Ti-6Al-4 V [3], most of them mainly focus on characteristics of tool wear and surface integrity while the effect of microstructure on cutting process was less reported. However, depending on the fabrication process, different microstructures (equiaxial, bimodal, and lamellae) of this alloy could be obtained yielding varying properties [1]. Even though in-depth studies have been conducted to analyze the effect of microstructure on material testing of titanium alloys (e.g., tensile, fatigue strength), only few research considered its effect on cutting performance, and most of these were limited to generic machining performances like tool wear and cutting forces [2–5]. Although some variation of chip morphology was observed before [5], the underlying mechanism was not discussed.

To better understand the machining induced deformation (material removal/chip formation) mechanism of titanium alloys, size effect is of great reference as the interaction between cutting tool and workpiece could vary when the undeformed chip thickness (UCT) reduces to grain size level [6,7] or even smaller [8]. This becomes even more complex in bimodal (dual-phase) Ti-6Al-4 V, since the equiaxed primary α (α_p) phase and lamellar α+β matrix (see Fig. 1a) show different mechanical properties [1].

As such, in this research, orthogonal cutting tests and numerical analysis were performed under different UCTs to reveal how the microstructure affects the deformation mechanism under small UCT (e.g. serration at phase boundary, Fig. 1b) while showing homogeneous properties at large UCT (see Fig. 1c).

Based on the results in chip morphologies, microstructures and subsurface deformation of machined workpieces, the change of material removal mechanism (i.e., from localized to uniformed chip serration) was analyzed and a new 'inverse size effect' of specific shear energy was revealed, which showed the influence of microstructure on cutting mechanism under different UCTs and could guide the optimization of suitable parameters for machining this material.

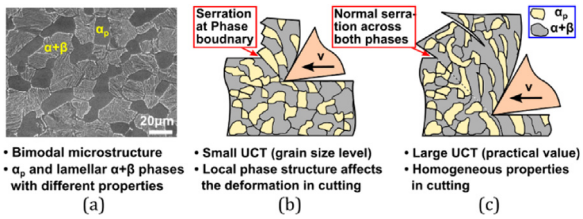

Fig. 1. Material microstructure and material removal mechanism of Ti-6Al-4 V. (a) Bimodal microstructure. (b) Serration at phase boundary under small UCT affected by the microstructure. (c) Uniformed chip serration across both phases under large UCT showing homogeneous properties.

2. Experimental details

In this study, orthogonal cutting experiments were performed on an in-house developed Pendulum-based Cutting Test (PbCT) setup [9] with carbide inserts (30° rake angle, 20 μm edge radius). Bimodal Ti-6Al-4 V (heat treated at 950 °C for 60 min + air cooled) containing primary α (α_p, 30 vol%) and lamellar α+β matrix with similar grain

* Corresponding author.
E-mail address: Zhirong.Liao@nottingham.ac.uk (Z. Liao).

https://doi.org/10.1016/j.cirp.2023.04.042

size (~30 μm) was used (see Fig. 1a). Three UCTs (50, 100, 150 μm) with cutting speed of 50 m/min and 1 mm cutting width were chosen. Numerical simulations of the chip formation and machined surface results were also performed with Abaqus by defining the different properties of two phases based on Johnson-Cook material models (see Table 1) [10].

Table 1
Johnson-Cook material models parameters of two phases [10].

Phase	Yield stress (MPa)	Strain hardening modulus (MPa)	Strain rate hardening coefficient	Thermal softening exponent	Strain hardening exponent
α_p	849.71	776.73	0.026	0.829	0.742
α+β	984.32	601.04	0.025	0.987	0.512

After the cutting tests, the obtained chips were examined by the scanning electron microscope - SEM (Quanta Q650) and Alicona G4 first. Then the chips and machined workpieces were prepared following metallurgical sample preparation and etching process. Advanced energy dispersive spectroscopy (EDS) and electron backscatter diffraction (EBSD) on JEOL 7100F were applied for in- depth analysis of microstructure deformation.

3. Results and discussion

3.1. Chip form and related deformation mechanism

The microstructure of machined chips was checked from the cross section (Fig. 2) to see whether the change of UCT from a large level (e.g. 100 μm [3]) to grain size level (e.g. 50 μm) could lead to different deformation mechanisms during cutting. Interestingly, although serrated chip form was generated in both cutting conditions, different formation mechanisms were noticed: (i) when UCT=50 μm, the serration tended to occur on the boundary between α_p and lamellar α+β due to the mismatch of mechanical properties between these two phases (around 40%) or within the softer lamellar α+β phase (see Fig. 2a); (ii) however, when UCT=100 μm, the serration with a much larger width occurred uniformly in the chip and both the α_p and lamellar α+β phases were sheared (Fig. 2b). These phenomena suggest a change of deformation mechanism for cutting Ti-6Al-4 V with bimodal microstructure, which is verified by the chip topography and more detailed cross-section results as described later.

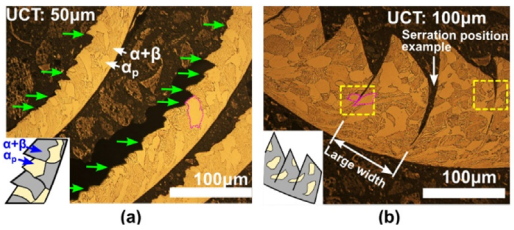

Fig. 2. Cross section of chips obtained under different undeformed chip thicknesses. (a) Serration tended to occur on phase boundary (indicated by green arrows) or softer lamellar α+β phase when UCT=50 μm. (b) Serration occurred uniformly and cut through both phases (in yellow rectangles) when UCT=100 μm. (For interpretation of the references to color in this figure legend, the reader is referred to the web version of this article.)

While serrated chips were obtained under all undeformed chip thicknesses, at close observation, the free surface of the chip showed quite different micro-topographical characteristics (see results in Figs. 3 and 4). For UCT=50 μm, localised serrations were formed on the free surface of the chip (Figs. 3b and 4a) which could be explained by the serration at phase boundary since the distance between serrations are close to phase size. With UCT increased to 100 μm, semicontinuous serrations occurred (Figs. 3d and 4b) due to less effect by the serration at phase boundary. At 150 μm UCT the free surface morphology of the chip presented continuous (layer by layer) serrations, as seen in Figs. 3f and 4c, regardless of local microstructure. While the continuous serration across the chip width [3] and smaller serration at lower UCT are widely reported in other work, the localized serration at small undeformed chip thickness what is shown to be dependant on metallurgical microstructure has not been studied yet.

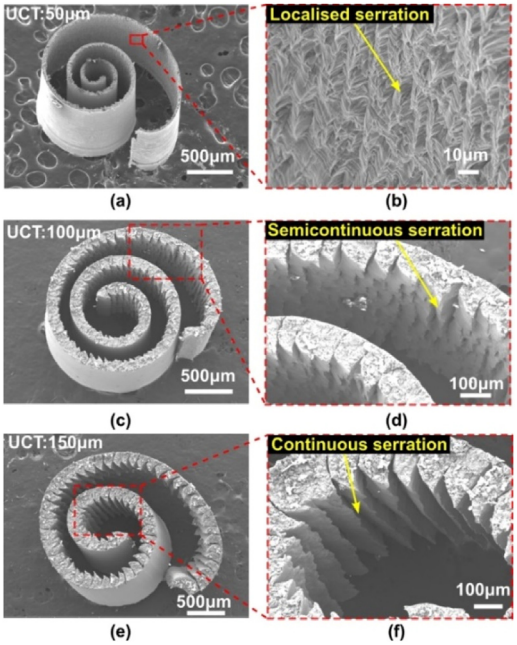

Fig. 3. Chip morphology on free surface under different UCTs. (a), (b) Chip from UCT=50 μm shows localized serrations at phase boundary. (c), (d) Chip from UCT=100 μm shows semicontinuous serrations due to less effect of serration at phase boundary. (e), (f) Chip from UCT=150 μm with continuous serration (layer by layer regular serration) regardless of local microstructure.

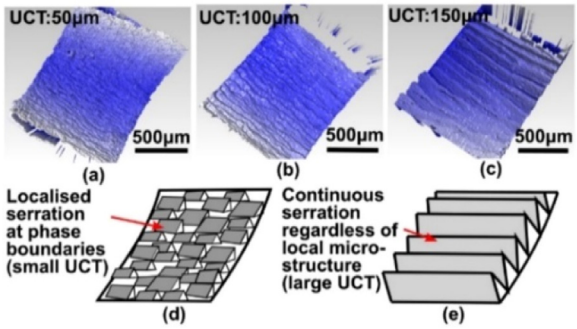

Fig. 4. Free surface topography and related schematics. (a)-(c) Free surface topography of the chips obtained from Alicona when UCT=50, 100, 150 μm. (d), (e) Schematics of the localised serration under small UCT vs. continuous serration under large UCT on free surface of the chips.

Based on these observations, more in-depth study on the crystalline microstructure of chips was performed by EDS and EBSD analysis (see Fig. 5). With the EDS results (V element), the phases in the material were clearly recognised while inverse pole figure (IPF) and kernel average misorientation (KAM) results offered information of grains and deformation distribution in the chips. As observed before, the EDS shows the change of serration position from boundaries between different phases at small UCT (localized serration) to the more uniformly distributed positions (regardless of local microstructure) at large UCT.

Combining the EDS information with the EBSD results, the details of deformation mechanism could be explained. With the UCT increasing, the misorientation in the chip changes from the relatively uniform distribution when UCT=50 μm (see Fig. 5c), to the localized large deformation near the shear bands at 150 μm UCT (see Fig. 5i),

Please cite this article as: S. Zan et al., Inverse size effect and deformation mechanism in Ti-6Al-4V cutting process – investigation on effect of bimodal microstructure on machining, CIRP Annals - Manufacturing Technology (2023), https://doi.org/10.1016/j.cirp.2023.04.042

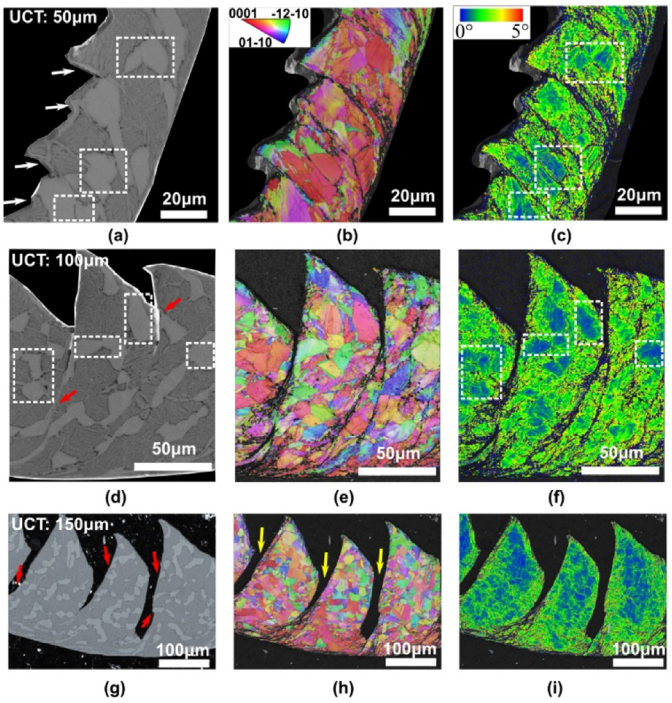

Fig. 5. EDS, IPF and KAM analysis of chips obtained under different UCTs showing the phases, grains, and deformation. (a)–(c) UCT=50 μm. (d)–(f) UCT=100 μm. (g)–(i) UCT=150 μm. Deformation is more uniformly distributed under lower UCT and α_p phase shows less deformation (white rectangles). The serration tends to occur at phase boundary at lower UCT (white arrow in (a)) while α_p phase can be cut through at larger UCT (red arrows in (d), (g)). (Cracks are indicated with yellow arrows in (h).). (For interpretation of the references to color in this figure legend, the reader is referred to the web version of this article.)

leaving low misorientation angle within the serrations. Moreover, the deformation occurring in α_p phase tended to be smaller than the one in the lamellar α+β (see low misorientation regions marked with white rectangles in Fig. 5c,f). This interesting aspect can be explained by the mechanical property mismatch of theses phases: bimodal microstructures can be considered to be a combination of lamellar and equiaxed microstructure, and the latter one (consist of α_p phase) shows higher strength than the former one (consist of lamellar α+β) [1]. Based on this, the lower misorientation angle in α_p phase could be attributed to its higher strength compared with lamellar α+β which leads to less deformation.

Regarding the serration position in the chips, while regular large serration (observed when UCT=100, 150 μm) was usually explained by crack generation (Fig. 5h) or the formation of adiabatic shear band where the material was weakened and slid (Fig. 5e), the serration positions at 50 μm UCT were affected by the local microstructure of the material. Since the strain are more uniformly distributed at small UCT (50 μm), the regions with less strength (phase boundary [11], lamellae α+β) are the "weak points" and initiate the serration.

To better understand the change of chip formation mechanism under different UCTs, a 2D finite element model was built with microstructure in cutting region (see Fig. 6). The grains were generated by Voronoi randomized algorithm with average grain size of 30 μm for both phases. Although the interface properties were not specifically defined, the different properties of two phases in FE model led to different deformation extent in two phases under small UCT while showing regular serration at large UCTs, which shows good correspondence between the experiment and simulation results in chips, and the change of deformation mechanism under different UCTs can be confirmed.

3.2. Deformation depth under machined surface

To evaluate the effect of UCTs on surface integrity and its relation to the microstructure, the cross section of machined surface was examined with the same procedure as chips (as shown in Fig. 7).

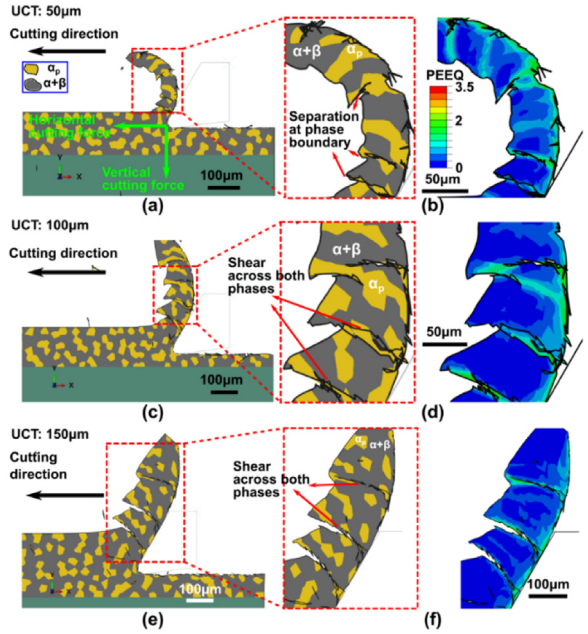

Fig. 6. Finite element modelling results of chip formation under different UCTs. (a), (c), (e) Microstructure of simulated chip when UCT=50, 100, 150 μm. (b), (d), (f) Enlarged figures of chips and related strain distribution.

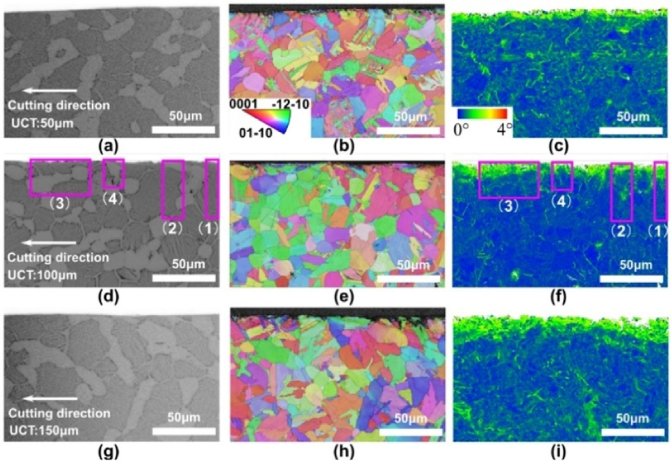

Fig. 7. EDS, IPF and KAM analysis of machined surface under different UCTs showing the phases, grains, and deformation. (a)-(c) UCT=50 μm. (d)–(f) UCT=100 μm. (g)–(i) UCT=150 μm. Deformation depth is affected by the microstructure in local area (4 typical conditions marked with pink rectangles in (d) and (f)).

Under the machined surface, swept grains could be observed and the deformation depth increased under larger UCT, indicating the severe plastic deformation in the workpiece. Apart from these widely reported phenomena, it was noticed that in this bimodal Ti-6Al-4 V, the deformation depth in the local area was also affected by its microstructure. To be specific, different phase strengths and their arrangements in the local area (4 conditions as described below) lead to different deformation depths under the same cutting parameters (see regions marked with pink rectangles in Fig. 7 and the schematic in Fig. 8a): (i) The local area only includes the lamellar phase - large deformation depth due to low strength of the lamellar phase; (ii) The α_p phase exists above the lamellar phase - the deformation transfers from the α_p phase to the lamellar phase; (iii) The lamellar phase exists above the α_p phase - the deformation tends to be blocked at the boundary of phases; (iv) The local area only includes the α_p phase - presenting smallest deformation depth due to the high strength of the α_p phase.

Although the strain distribution on simulated machined surface was too small to analyse, the obtained stress results could help

Please cite this article as: S. Zan et al., Inverse size effect and deformation mechanism in Ti-6Al-4V cutting process – investigation on effect of bimodal microstructure on machining, CIRP Annals - Manufacturing Technology (2023), https://doi.org/10.1016/j.cirp.2023.04.042

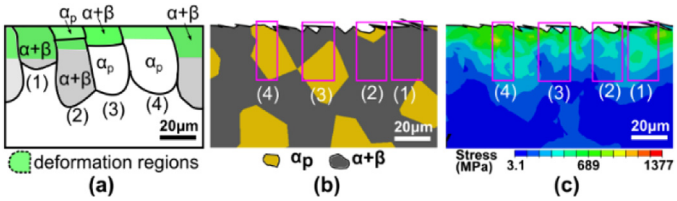

Fig. 8. Schematic and simulation results of subsurface. (a) Schematic of deformation depth with 4 typical microstructures in local area. (b) Microstructure of simulated machined surface when UCT=50 μm. (c) Simulated stress distribution under machined surface when UCT=50 μm.

interpret the microstructure affected deformation depth (see Fig. 8b, c). From these, the stress variation at phase boundaries could be recognized and the shallower stress distribution depth under lamellar phase were observed, showing the efficient stress absorption ability of this soft phase by deformation.

3.3. Inverse size effect of shear energy per unit volume

Based on the previous analysis, it is discovered that the microstructure of bimodal Ti-6Al-4 V can change the deformation mechanism in cutting process under different UCTs. To further evaluate its effects, total, shear and friction energies per unit volume (specific energies) were calculated by the average values of cutting forces and chip thickness [2] from experiment and simulation results (see Table 2 and Fig. 9). Considering ploughing and extruding effects, the material volume above stagnation point was used for the calculation of specific energies and ploughing force was subtracted in the calculation.

Table 2
Cutting force and chip thickness under different UCTs.

Undeformed chip thickness (μm)		50	100	150
Experiment	Horizontal cutting force (N)	92.8	163.2	208.6
	Vertical cutting force (N)	41.5	40.2	30.7
	Chip thickness (μm)	53.0	141.8	252.4
Simulation	Horizontal cutting force (N)	107.7	181.9	271.0
	Vertical cutting force (N)	66.5	60.6	46.6
	Chip thickness (μm)	65.2	127.8	208.0

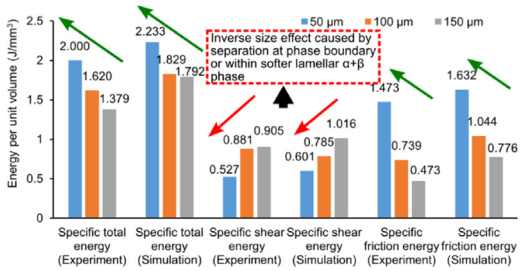

Fig. 9. Specific energies under different UCTs.

According to the energy analysis, the specific total and friction energies showed an increasing trend as the UCT decreased (size effect), while the specific shear energy did the opposite (inverse size effect). Despite the size effect in specific total energy and increase of friction effect at smaller UCT were widely reported [6], the opposite trend of specific shear energy was not expected as it did not match the trend of shear stress increase with reduced UCT reported before for other material [6]. However, this can be explained by the change of deformation mechanism mentioned before: in the experiment and simulation results (Figs. 5 and 6), it is noticed that the serrations in chips at larger UCTs (100 μm, 150 μm) are more regularly distributed with the cracks crossing both kinds of phases. However, at smaller UCT (50 μm), the localised serration tends to occur at the phase boundaries or within the lamellar α+β where the required energy for crack propagation is smaller and eventually leads to reduced specific shear energy when forming the chip and shows an 'inverse size effect' in cutting this bimodal Ti-6Al-4 V.

4. Conclusion

This paper reports a curious observation of the deformation mechanism in Ti-6Al-4 V machining whereby the bimodal microstructure can affect the size effect occurred in cutting process. With an in-depth investigation on the orthogonal cutting results, the change of deformation mechanism induced by the phase property mismatch is discovered. When forming the chip, the regular serration is replaced by the serration at phase boundary or within softer lamellar α+β phase under small UCT, which in turn leads to the 'inverse size effect' in cutting process - reduction of specific shear energy with UCT decrease. Based on the strength of the two different phases in the material, the deformation depth on subsurface of machined workpieces is analyzed and concluded to 4 typical conditions (single lamellar phase, single α_p phase, lamellar above α_p phase, and α_p above lamellar phase) according to the local microstructure. From this research, it can be concluded that the shear deformation of this material is easier under smaller UCT. If appropriate parameters, e.g. UCT and tool edge radius (to reduce ploughing effect at smaller UCT), are applied, easier material removal and better surface integrity could be achieved which is of great guidance value in practical machining.

Declaration of Competing Interest

The authors declare that they have no known competing financial interests or personal relationships that could have appeared to influence the work reported in this paper.

References

[1] Leyens C, Peters M (2003) *Titanium and Titanium Alloys: Fundamentals and Applications*, Wiley.
[2] Shaw MC (2005) *Metal Cutting Principles*, Oxford University Press; New York.
[3] M'Saoubi R, Axinte D, Soo SL, Nobel C, Attia H, Kappmeyer G, Engin S, Sim WM (2015) High performance cutting of advanced aerospace alloys and composite materials. *CIRP Ann.* 64(2):557–580.
[4] Ahmadi M, Karpat Y, Acar O, Kalay YE (2018) Microstructure effects on process outputs in micro scale milling of heat treated Ti6Al4V titanium alloys. *J. Mater. Process. Technol.* 252:333–347.
[5] Cedergren S, Petti G, Sjöberg G (2013) On the influence of work material microstructure on chip formation, cutting forces and acoustic emission when machining Ti-6Al-4V. *Procedia CIRP* 12:55–60.
[6] Fu MW, Wang JL (2021) Size effects in multi-scale materials processing and manufacturing. *Int. J. Mach. Tools Manuf.* 167:103755.
[7] Axinte D, Huang H, Yan J, Liao Z (2022) What micro-mechanical testing can reveal about machining processes. *Int. J. Mach. Tools Manuf.* 183:103964.
[8] Fang F, Lai M, Wang J, Luo X, Yan J, Yan Y (2022) Nanometric cutting: mechanisms, practices and future perspectives. *Int. J. Mach. Tools Manuf.* 178:103905.
[9] Xu D, Liao Z, Axinte D, Hardy M, M'Saoubi R (2019) A quick method for evaluating the thresholds of workpiece surface damage in machining. *CIRP Ann.* 68(1):61–64.
[10] Ren Y, Ma Y, Pan Q (2020) Effect of Microstructure on the Johnson-Cook constitutive model parameters of Ti-6Al-4V Alloy. *J. Phys. Conf. Ser.* 1637(1):012018.
[11] Kim JH, Semiatin SL, Lee CS (2005) Constitutive analysis of the high-temperature deformation mechanisms of Ti–6Al–4V and Ti–6.85Al–1.6V alloys. *Mater. Sci. Eng. A* 394(1–2):366–375.

Please cite this article as: S. Zan et al., Inverse size effect and deformation mechanism in Ti-6Al-4V cutting process – investigation on effect of bimodal microstructure on machining, CIRP Annals - Manufacturing Technology (2023), https://doi.org/10.1016/j.cirp.2023.04.042